Dynamic Nuclear Polarization of ^{29}Si Nuclei Induced by Li and Li–O Centers in Silicon

Mohammad R. Rahman*, Tatsumasa Itahashi, Marina P. Vlasenko[1], Leonid S. Vlasenko[1], Eugene E. Haller[2], and Kohei M. Itoh

School of Fundamental Science and Technology, Keio University, Yokohama 223-8522, Japan
[1]*A. F. Ioffe Physico-Technical Institute, 194021 St. Petersburg, Russia*
[2]*Lawrence Berkeley National Laboratory and UC Berkeley, 1 Cyclotron Rd., Berkeley, CA 94720, U.S.A.*

Received June 4, 2010; accepted July 23, 2010; published online October 20, 2010

Dynamic nuclear polarization (DNP) of ^{29}Si nuclear spins induced by saturation of electron paramagnetic resonance (EPR) transitions of lithium-related centers in float zone (FZ) grown silicon is reported. Both isolated Li and Li–O complex centers showed strong EPR absorption lines in the temperature range 3.4–10 K and led to very efficient orientation of ^{29}Si nuclear spins. The temperature dependence and time constant of ^{29}Si DNP are investigated in detail. The ^{29}Si DNP of 0.72% was achieved at 3.4 K by excitation of the Li–O forbidden EPR transition under illumination, corresponding to a ~352 fold increase with respect to the thermal equilibrium polarization.

DOI: 10.1143/JJAP.49.103001

1. Introduction

Silicon spintronics has been attracting much attention since the proposal of a silicon-based quantum computer by Kane.[1)] More recently, a proposal of utilizing ^{29}Si nuclei as qubits emerged[2,3)] in order to take advantage of the long coherence time of ^{29}Si nuclear spins.[4)] One of the major challenges involving a nuclear spin as a qubit is the difficulty in initialization, i.e., achieving the spin polarization of at least 5% needed at the beginning of quantum computing for application of the efficient algorithmic cooling protocol.[5)] Dynamic nuclear polarization (DNP) is one of several promising methods to achieve such a high degree of the ^{29}Si nuclear polarization by transferring the equilibrium Boltzmann electron polarization to nuclei. Obtaining high nuclear polarization by DNP requires low temperatures and strong magnetic fields. Previously carried out DNP experiments with phosphorus doped silicon achieved ^{29}Si polarization of 1.45% but this was limited by the long relaxation time of electrons bound to phosphorus donors ($\approx 3 \times 10^3$ s at 1.2 K)[6)] that did not allow efficient DNP at low temperatures ($T < 10$ K).[7,8)] Much shorter spin–lattice relaxation time expected for electrons bound to Li in silicon at $T < 10$ K makes Li an attracting candidate as a ^{29}Si DNP mediator.

The methods of DNP were established by Overhauser,[9,10)] Jeffries,[11)] and Abragam[12,13)] as extensions of earlier static methods.[14,15)] DNP occurs by mutual electron–nuclear spin flipping mediated by hyperfine interaction between nuclear and electron spins. As shown in Fig. 1, DNP via excitation of allowed and forbidden electron paramagnetic transition corresponds to the *Overhauser effect* and the *solid effect*, respectively. However, which one of the two mechanisms becomes more effective depends on the nature of the system. It was found for phosphorus in silicon that the *solid effect* is actually much more effective then *Overhauser effect* when the phosphorus concentration N(P) is less than 5×10^{16} cm^{-3} and *vice versa*.

The DNP of the ^{29}Si nuclei was demonstrated for the first time by Abragam in silicon doped with phosphorus $N(\mathrm{P}) \approx 5 \times 10^{16}$ cm^{-3}. The DNP enhancement of $E = 30$ corresponding to a nuclear polarization of 0.048% was observed under saturation of the phosphorus electron paramagnetic resonance (EPR) lines by microwave field at 4.2 K.[16)] Much lower DNP enhancement of $E = 4.6$ was observed in similar silicon crystals at 6 K but very high $E = 2680$ corresponding to nuclear polarization 1.45% was achieved at 12 K in an isotopically enriched crystal containing only 1% of ^{29}Si nuclear spins.[7,8)]

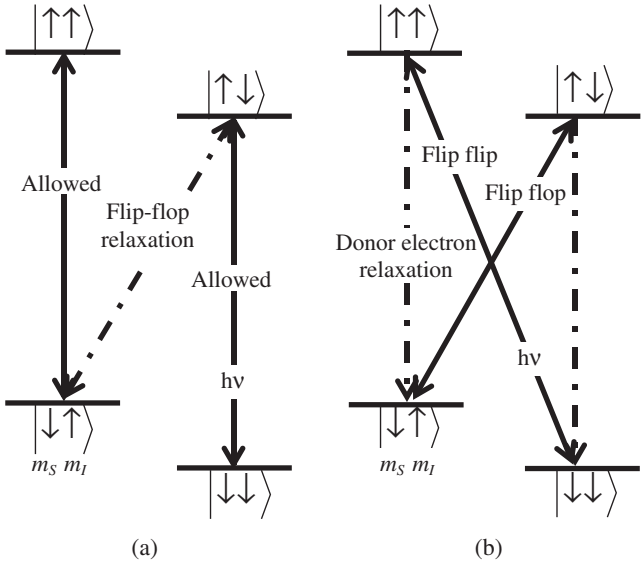

Fig. 1. Typical mechanisms of dynamic nuclear polarization (DNP) of ^{29}Si nuclear spins ($I = 1/2$) in silicon utilizing the interaction with electron spins ($S = 1/2$). Left and right arrows in each ket represent orientation of electron and ^{29}Si nuclear spins, respectively. (a) *Overhauser effect* involves saturation of allowed electron spin transitions ($\Delta m_S = \pm 1$, $\Delta m_I = 0$, where m_S and m_I are the magnetic quantum number of electron and nucleus spins, respectively) leading to electron spin flip alone at the time of excitation. Subsequent flip-flop relaxation between the electron spin and ^{29}Si nuclear spin that are coupled by contact hyperfine interacton gives rise to polarization of the ^{29}Si nuclei. (b) *Solid effect* involves saturation of forbiden transitions [flip-flop ($\Delta m_S + \Delta m_I = 0$) or flip-flip ($\Delta m_S + \Delta m_I = \pm 2$)] leading to flipping of electron and nuclear spins together. Subsequent relaxation of the electron orients ^{29}Si nuclei polarization in either an up or a down direction.

Among a variety of shallow donors in silicon the neutral interstitial lithium (Li^0) is unique because its A_1 state is 1.8 meV higher than ground fivefold degenerated $T_2 + E$ state unlike the case of phosphorus in which $T_2 + E$ state is 12 meV higher than A_1 state.[17,18)] The degeneracy of the ground state of lithium in silicon gives rise to a nontrivial spin-orbit coupling[19)] and such an inverted level structure

*E-mail address: rizwan.mme@gmail.com

and the degeneracy of Li ground state lead to short electron spin–lattice relaxation time $T_{1e} = 12\,\mu s$ at $T = 2.1\,K$ and $1.5\,\mu s$ at $T = 4.5\,K$.[20] Such a short relaxation time led to the experimental observation of DNP of ^{29}Si at $T = 3.4\,K$ using isolated Li^0.[21]

The present paper investigates DNP of ^{29}Si nuclei in float-zone (FZ) silicon containing paramagnetic Li^0 donors and lithium+oxygen (Li–O) centers. The dependences of the ^{29}Si DNP degree on the temperature, illumination, and externally applied magnetic field direction are investigated.

2. Experimental Procedure

A FZ-silicon crystal grown in ⟨100⟩ direction having 2000 Ω cm resistivity was used for Li diffusion at 420 °C in vacuum for 15 min. The silicon wafers were mechanically polished before diffusion with 1900 mesh size slurry. After diffusion some of the samples were annealed for 45 min at 450 °C in vacuum. The concentrations of free electrons at room temperature determined by Hall measurements were $\approx 10^{16}\,cm^{-3}$ for all samples.

EPR spectra were recorded with an *X*-band JEOL EPR spectrometer. The temperature of samples was controlled by an Oxford Instruments He gas flow cryostat in the range of 3.2–50 K. A 100 W halogen lamp was used for illumination of the sample. The lamp contains the wavelength of 1048 nm and shorter that corresponds to above band gap illumination for silicon. The penetration depth at 1048 nm is about 20 mm, i.e., we assume such band edge illumination to penetrate through the sample.[22] For accurate determination of the *g*-values of observed EPR lines, the detection of EPR spectra was performed together with the reference silicon sample containing 5×10^{16} phosphorus atoms having well known isotropic *g*-value of 1.9985 ± 0.0001.

The DNP of the ^{29}Si nuclei were performed using the EPR spectrometer for saturating the EPR lines at the microwave power optimal for each sample typically in the range of 20–200 mW. The time *t* of saturation (microwave irradiation) was varied between 10 min and 10 h. The sample transfer from electron paramagnetic resonance (EPR) to nuclear magnetic resonance (NMR) spectrometers was performed with a disc permanent magnet placed on top of the sample to avoid the fast nuclear spin lattice relaxation in zero magnetic field. The DNP degree was determined by comparing the intensity of a NMR signal after saturation of the EPR line with respect to the equilibrium NMR signal recorded at room temperature and a magnetic field of 7 T. The details of DNP experiments and measurements of DNP degree were described in ref. 7.

3. Results and Discussion

3.1 EPR spectra

EPR spectra observed in silicon after diffusion of Li atoms at 450 °C for 15 min are shown in Fig. 2. The angular dependence of this EPR spectrum (not displayed) shows an axially symmetric *g*-tensor about ⟨100⟩ with the components $g_{\parallel} = g_{[100]} = 1.9996 \pm 0.0001$ and $g_{\perp} = 1.9986 \pm 0.0001$, which are in good agreement with the previously reported values for neutral Li atoms (Li^0) occupying tetrahedral interstitial positions.[23] This signal can be detected at temperatures below 20 K and its intensity continues to increase all the way down to 3.4 K, which was the lowest temperature employed in this study. This situation is in sharp contrast to the EPR of electrons bound to phosphorus whose intensity maximum situates around 12 K and becomes undetectable at lower temperatures due to an increase of T_{1e}, i.e., the relaxations shown in Fig. 1 hardly occur. It should be noted that the EPR spectra shown in Fig. 2 are recorded without application of external stress that was needed to obtain such spectra in the earlier studies.[23] The existence of uniaxial stress in the direction perpendicular to the silicon surface after mechanical grinding was demonstrated previously.[25,26] However, we observe the signal shown in Fig. 2 even after sufficient chemical etching of the surfaces to remove such stress. The clear observation of the isolated Li centers without external stress makes our DNP experiments very straightforward.

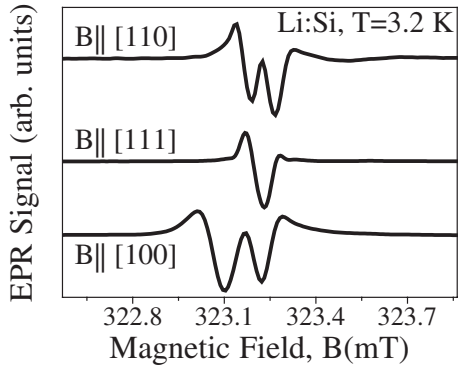

Fig. 2. EPR spectra of Li^0 centers detected in the second derivative mode with different orientation of the externally applied magnetic field B indicated in the figure.

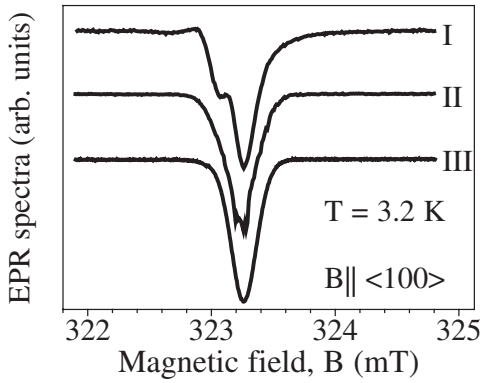

Fig. 3. EPR spectra detected in the second derivative of absorption mode: (I) immediately after 45 min annealing at 450 °C, (II) after 2 days, and (III) after 4 weeks. The peak (III) arises from Li–O complexes for the reasons described in the text.

Additional EPR lines emerge in the Li diffused samples immediately after annealing at 450 °C for 45 min labeled (I) in Fig. 3. Moreover, these EPR centers are not stable at room temperature and change their character over the time period of days and are labeled (II) and (III) in Fig. 3. One broad and stable peak labeled (III) is used for further analysis and DNP. The variation of this broad line at different orientations of the annealed crystal in the magnetic field (not shown) agrees with those indentified as Li–O complex in ref. 24.

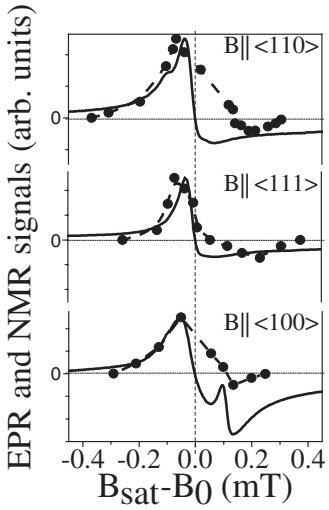

Fig. 4. The increased (>0) or decreased (<0) ^{29}Si NMR signal intensities (●) after saturation of the Li^0 EPR transition in the magnetic field given by the horizontal axis and the direction indicated in the figure. The horizontal axis shows the deviation of the magnetic field B_{sat} from the field B_0 that gives the maximum of Li^0 EPR line. The solid curves show the first derivative of the Li^0 EPR absorption lines. The ^{29}Si NMR signals were acquired at $T = 300$ K and $B = 7$ T after microwave saturation with microwave power of 200 mW during 10 min at $T_s = 3.4$ K. The positive and negative signs of the NMR signals correspond to DNP in the opposite and the same directions with respect to equilibrium nuclear polarization.

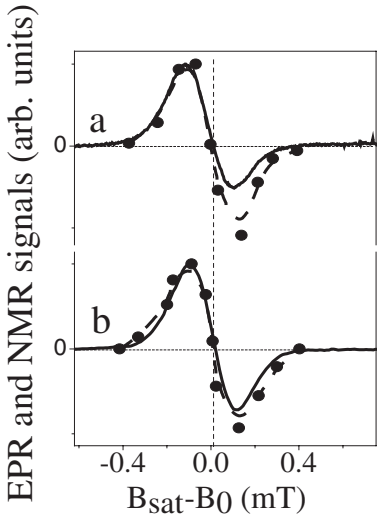

Fig. 5. The dependences of the ^{29}Si DNP after 10 min of EPR line saturation on the deviation of the magnetic field B_{sat} from the center of the Li–O EPR line B_0 (●) and the first derivative of the EPR line (solid lines) without (a) and under (b) illumination at the orientation of magnetic field along ⟨100⟩ crystal axis.

The variation of the EPR spectra with the time after the second annealing can be related to slow relaxation of lattice stress in the sample and, probably, to slow but mobile Li even at room temperature after the second annealing. Li atoms may tend to stabilize themselves near oxygen to form Li–O complexes. The concentration of paramagnetic Li–O centers estimated from the EPR line intensities is around $2 \times 10^{16}\,cm^{-3}$ which is below the typical concentration $5 \times 10^{16}\,cm^{-3}$ of oxygen in FZ silicon.

3.2 Dynamic nuclear polarization

DNP of ^{29}Si nuclear spins was observed in all of the investigated samples under saturation of EPR lines of both the Li^0 and Li–O centers. Figure 4 shows the enhanced ^{29}Si NMR signal intensities (solid circles) after saturation of the Li^0 EPR transition in the magnetic field given by the horizontal axis. Figure 4 also shows the EPR lines intensity (solid curve) for comparison. Figure 5 shows the same plot for the Li–O complexes.

As shown in Fig. 1(a), the peaks in the ^{29}Si NMR intensity should appear at $B_{sat} - B_0 = 0$ if the *Overhauser effect* is dominant. The fact that this not the case in both Figs. 4 and 5 gives clear evidence that the DNP of ^{29}Si nuclei is the result of the *solid effect*. The shift, $\Delta B_{\pm}$, of the forbidden "flip-flop" and "flip-flip" transitions from the center of EPR line ($B_0 \cong 323$ mT) is approximately $\Delta B_{\pm} = B - B_0 = \pm B_0(\gamma_n/\gamma_e) \approx \pm 0.1$ mT for the ^{29}Si nuclei. Indeed, for the case of the DNP with Li^0 centers, the spacing between maximal positive and negative DNP-NMR signals slightly exceeds the Li^0 EPR linewidth that is narrower than 0.2 mT. This is a typical case of the so-called partly resolved solid-effect,[27] where forbidden flip-flop and flip-flip transitions occur at the magnetic field just outside of the EPR linewidth. This explains why the dependence of the DNP NMR signals does not follow exactly the EPR first derivative line-shape of the Li^0 center (Fig. 4). On the other hand the EPR linewidth of the Li–O center is much larger than that of Li^0 and the NMR intensity shape agrees very well with the EPR first derivative line-shape (Fig. 5). In this case the flip-flop and flip-flip transitions are buried within the linewidth of the inhomogeneously broadened EPR peak.

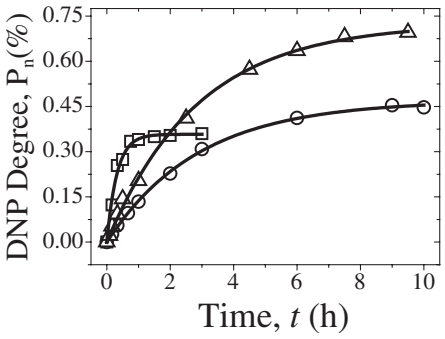

Fig. 6. The DNP degree, P_n, vs EPR saturation time, t, obtained without illumination at $T = 3.4$ K in the samples containing Li^0 (□) and Li–O (○) centers and in the sample with Li–O center under illumination (△).

The ^{29}Si NMR signals detected after DNP were 10^2–10^3 times stronger than the signal detected from the control sample, i.e., the same sample without DNP but after keeping it in the magnetic field of 7 T at room temperature for 10–20 h. In this case the equilibrium Boltzmann nuclear polarization is $P_{n0} \cong 4.8 \times 10^{-4}$%. The increase of NMR signals with the DNP time (t), i.e., duration of saturation in the EPR spectrometer, is shown in Fig. 6. These dependences are exponential and allow us to determine the nuclear polarization time T_{1n} and DNP degree P_n^{ss} by the extrapolation of the curves to the infinite saturation time. Such values for the lowest temperature obtained in this study $T = 3.4$ K are summarized in the Table I. The DNP enhancement E^{ss} was determined with respect to the

Table I. Summary of the ^{29}Si nuclear polarization time T_{1n}, DNP degree P^{ss} obtained by extrapolation to infinite saturation time, and DNP enhancement E^{ss} for different investigated samples.

Sample	T (K)	Orientation	T_{1n} (h)	P_n^{ss} (%)	E^{ss}
Si:Li Isolated Li^0	3.4	⟨100⟩	0.35	0.17	85
		⟨111⟩	0.33	0.35	170
		⟨110⟩	0.4	0.28	97
Si:Li Li–O complex (dark)	3.4	⟨100⟩	3.0	0.46	225
		⟨110⟩	3.5	0.29	145
Si:Li Li–O complex (light)	3.4	⟨100⟩	3.0	0.72	352
		⟨110⟩	2.7	0.48	235
Si:P (10^{16} cm^{-3})[a)]	12	—	1.2	0.28	511

a) The data are taken from ref. 8. At 3.4 K the DNP in Si doped with phosphorus was not observed.

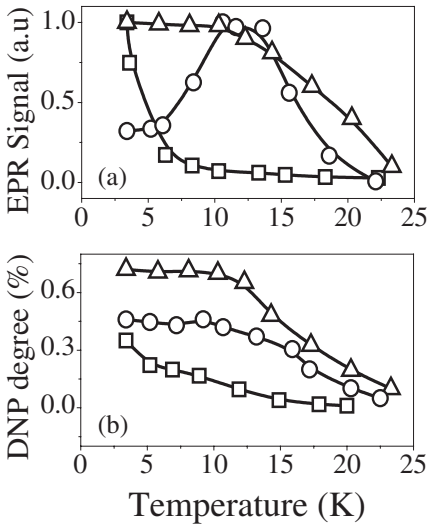

Fig. 7. The dependences of the (a) EPR line amplitudes and (b) DNP degree on the temperature of samples containing Li^0 (□) and Li–O (○) centers under dark and with illumination for Li–O center (△).

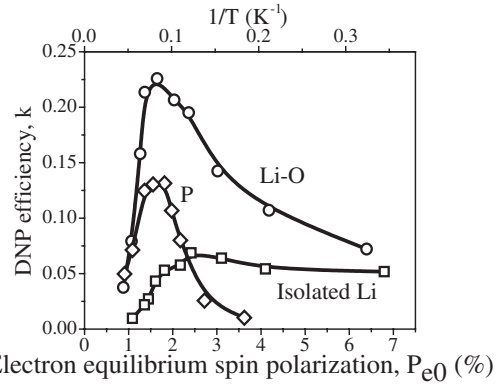

Fig. 8. The DNP efficiency k, vs equilibrium electron spin polarization degree P_{e0}, for samples containing Li^0 (□), Li–O (○), and phosphorus (◇) under dark.

equilibrium nuclear spin polarization in the same magnetic field (≈323 mT). The Li–O complex EPR intensity is twice as high under band gap illumination compared to in dark for the temperature range 3.4–10 K. The possible reasons for the change in EPR intensity are the increase in the absorption rate due to reduction in T_{1e} and enhancement in the Li–O donor concentration under illumination. Due to reduction in T_{1e}, fast mutual flipping of electron and ^{29}Si nuclear spin under saturation of forbidden transitions increases the effective DNP degree. The DNP degree also depends on the leakage factor which is proportional to T_{1e}.[27] Therefore the maximum DNP degree obtained in this study $P_n^{ss} = 0.72\%$ was achieved at 3.4 K using Li–O EPR saturation of forbidden transition performed with halogen lamp illumination. The enhanced DNP degree under illumination was the combine effect of the reduced T_{1e} and donor concentration increment.

A ten times shorter nuclear polarization time T_{1n} observed in the samples containing Li^0 centers in comparison with the DNP caused by Li–O (Table I) can also be attributed to shorter electron spin–lattice relaxation time T_{1e} of Li^0. The nuclear relaxation rate $1/T_{1n}$ is proportional to the concentration of paramagnetic centers N and to $1/T_{1e}$.[8,14,27] Because concentrations of paramagnetic centers in our samples are approximately the same, the nuclear polarization time is determined by the electron spin-relaxation time which is shorter for Li^0 centers.

Figure 7 shows the temperature dependence of the EPR signal amplitudes and DNP degrees P_n^{ss} for different samples. In contrast to the DNP utilizing phosphorus donors, the EPR spectra of both the isolated Li and Li–O centers are detected at temperatures well below 10 K.

Below 10 K, the EPR intensity of the isolated Li increases whereas that of Li–O centers decreases. The temperature dependence of the Li–O EPR intensity is similar to that of phosphorus and is explained by longer electron spin–lattice relaxation time T_{1e} than that for Li^0 centers.[8] This is confirmed by the lower microwave power needed to saturate the Li–O EPR spectrum than those needed for the Li^0 EPR spectrum. As can be seen in Fig. 7, shortening T_{1e} under illumination increases the EPR intensity of Li–O centers below 10 K. However, illumination does not affect the Li^0 EPR spectrum. The temperature dependence of the DNP degree for different samples correlates well with the temperature dependences of the intensity of EPR spectra [see Fig. 7(b)].

The efficiency of DNP can be defined as the degree of the equilibrium electron spin polarization that is transferred to nuclear spins by the DNP process, i.e., $k = P_n/P_{e0}$. Figure 8 shows the dependence of k on the equilibrium electron polarization, which depends linearly on $1/T$ for all the experimental conditions ($B = 320$ mT, $T = 3.4$–20 K). The DNP efficiency using phosphorus (ref. 8) is shown for comparison. The DNP degree of Li–O complex in the temperature range 3.4–10 K [Fig. 7(b)] is higher than those of phosphorus and isolated Li as listed in Table I. This reflects the highest DNP efficiency of Li–O at 10 K because P_{e0} decreases exponentially with increasing temperature. The decrease in the DNP efficiency of Li–O at $T < 10$ K is due to the increase of the electron spin lattice relaxation time. The decrease in the efficiency of Li–O at $T > 10$ K is caused by ionization of the shallow donor levels.

3.3 Towards further improvement of DNP using Li related center

We have observed that EPR spectrum of the Li related center was not fully saturated at 200 mW microwave power due to its short T_{1e} and the EPR line showing inhomogeneous broadening characteristics. So, it would be desirable to use higher microwave power to saturate transitions, which would help to achieve higher nuclear spin polarizations and lower nuclear polarization time (T_{1n}). Moreover, the differential solid effect due to inhomogeneous broadening reduces the polarization in our system,[27] which can be overcome by using *integrated solid* effect[28] (ISE) or by the *nuclear spin orientation via electron spin locking* (NOVEL) method.[29] NOVEL can be more effective than ISE for Li related centers due to its short T_{1e}. On the other hand, broadening of the Li^0 EPR lines is caused by random internal stress. By applying external uniaxial stress the Li^0 EPR line width can be reduced significantly and a higher DNP can be achieved.[23]

^{28}Si isotopically enrich samples can also be used to eliminate the inhomogeneous broadening of the EPR lines of Li related centers. We can also achieve higher polarization of ^{29}Si using samples with donor concentration $\sim 10^{17}\,\mathrm{cm}^{-3}$, as shown by Dementyev *et al.* where they have reported $10.0 \pm 3.4\%$ ^{29}Si polarization by donor electrons via the Overhauser mechanism within exchange-coupled donor clusters in phosphorus and antimony doped single crystal silicon.[30] Lithium can be a good candidate for the above mechanism as its short electron spin lattice relaxation time allows for working at much lower temperatures. Higher magnetic fields at lower temperatures lead to higher electron polarization that can interact with ^{29}Si nuclei.

4. Conclusions

The EPR spectrum of the Li related donor center in FZ Si was observed in the 3.4–20 K range under absorption mode which led to the conclusion that Li had a shorter electron spin lattice relaxation time than that of phosphorus. The field dependence of ^{29}Si nuclei polarization was investigated in detail to show that the DNP was dominated by the solid effect for both neutral Li and Li–O complex centers. Higher DNP of ^{29}Si nuclei produced by Li^0 centers than those by phosphorus was observed at low temperature (3.4 K). Saturation of the Li–O complex EPR transition under illumination gives a 352 fold enhancement and 0.72% polarization of ^{29}Si nuclei.

Acknowledgements

This work was supported in part by a Grant-in-Aid for Scientific Research of Specially Promoted Research (18001002) from the Ministry of Education, Culture, Sports, Science and Technology, in part by Special Coordination Funds for Promoting Science and Technology, in part by JST-DFG Strategic Cooperative Program on Nanoelectronics, in part by the Funding Program for World-Leading Innovative R&D on Science and Technology FIRST, and in part by a Grant-in-Aid for the Global Center of Excellence at Keio University.

1) B. E. Kane: Nature (London) **393** (1998) 133.
2) K. M. Itoh: Solid State Commun. **133** (2005) 747.
3) T. D. Ladd, J. R. Goldman, F. Yamaguchi, Y. Yamamoto, E. Abe, and K. M. Itoh: Phys. Rev. Lett. **89** (2002) 017901.
4) T. D. Ladd, D. Maryenko, Y. Yamamoto, E. Abe, and K. M. Itoh: Phys. Rev. B **71** (2005) 014401.
5) L. J. Schulman and U. V. Vazirani: Proc. 31st ACM Symp. Theory of Computing, 1999, p. 322.
6) G. Feher and E. A. Gere: Phys. Rev. **114** (1959) 1245.
7) H. Hayashi, T. Itahashi, K. M. Itoh, L. S. Vlasenko, and M. P. Vlasenko: Phys. Rev. B **80** (2009) 045201.
8) H. Hayashi, W. Ko, T. Itahashi, A. Sagara, K. M. Itoh, L. S. Vlasenko, and M. P. Vlasenko: Phys. Status Solidi C **3** (2006) 4388.
9) A. W. Overhauser: Phys. Rev. **89** (1953) 689.
10) A. W. Overhauser: Phys. Rev. **92** (1953) 411.
11) C. D. Jeffries: Phys. Rev. **106** (1957) 164.
12) A. Abragam: Phys. Rev. **98** (1955) 1729.
13) A. Abragam: *The Principles of Nuclear Magnetism* (Clarendon Press, Oxford, U.K., 1961) p. 354.
14) C. J. Gorter: Physica **14** (1948) 504.
15) M. E. Rose: Phys. Rev. **75** (1949) 213.
16) A. Abragam, J. Combrisson, and I. Solomon: C. R. Acad. Sci. **247** (1958) 2337.
17) R. L. Aggarwal, P. Fisher, V. Mourzine, and A. K. Ramdas: Phys. Rev. **138** (1965) A882.
18) C. Jagannath and A. Ramdas: Phys. Rev. B **23** (1981) 4426.
19) V. N. Smelyanskiy, A. G. Petukhov, and V. V. Osipov: Phys. Rev. B **72** (2005) 081304(R).
20) V. N. Smelyanskiy, A. G. Petukhov, A. M. Tyryskin, S. A. Lyon, T. Schenkel, J. W. Ager, and E. E. Haller: arXiv:0807.3928.
21) M. R. Rahman, L. S. Vlasenko, E. E. Haller, and K. M. Itoh: Physica B **404** (2009) 5060.
22) G. G. Macfarlane, T. P. McLean, J. E. Quarrington, and V. Roberts: Phys. Rev. **111** (1958) 1245.
23) G. D. Watkins and F. S. Ham: Phys. Rev. B **1** (1970) 4071.
24) G. Feher: Phys. Rev. **114** (1959) 1219.
25) M. Höhne: Phys. Status Solidi B **86** (1978) 119.
26) P. Fisher and R. E. M. Vickers: Appl. Phys. Lett. **79** (2001) 3458.
27) O. S. Leifson and C. D. Jeffries: Phys. Rev. **122** (1961) 1781.
28) A. Henstra, P. Dirksen, and W. Th. Wenckebach: Phys. Lett. A **134** (1988) 134.
29) A. Henstra, P. Dirksen, J. Schmidt, and W. Th. Wenckebach: J. Magn. Resonance **77** (1988) 389.
30) A. E. Dementyev, D. G. Cory, and C. Ramanathan: arXiv:0903.4699v2.